Oncogene (2000) 19, 5303–5313

www.nature.com/onc

IC261, a specific inhibitor of the protein kinases casein kinase 1-delta and -epsilon, triggers the mitotic checkpoint and induces p53-dependent postmitotic effects

L Behrend[1], DM Milne[2], M Stöter[1], W Deppert[1], LE Campbell[2,3], DW Meek[2] and U Knippschild*[,1]

[1]*Heinrich-Pette-Institut für Experimentelle Virologie und Immunologie, Martinstrasse 52, D-20251 Hamburg, Germany;*
[2]*Biomedical Research Centre, Ninewells Hospital and Medical School, University of Dundee, Dundee DD1 9SY, UK*

The p53-targeted kinases casein kinase 1δ (CK1δ) and casein kinase 1ε (CK1ε) have been proposed to be involved in regulating DNA repair and chromosomal segregation. Recently, we showed that CK1δ localizes to the spindle apparatus and the centrosomes in cells with mitotic failure caused by DNA-damage prior to mitotic entry. We provide here evidence that 3-[(2,4,6-trimethoxyphenyl)methylidenyl]-indolin-2-one (IC261), a novel inhibitor of CK1δ and CK1ε, triggers the mitotic checkpoint control. At low micromolar concentrations IC261 inhibits cytokinesis causing a transient mitotic arrest. Cells containing active p53 arrest in the postmitotic G1 phase by blockage of entry into the S phase. Cells with non-functional p53 undergo postmitotic replication developing an 8N DNA content. The increase of DNA content is accompanied by a high amount of micronucleated and apoptotic cells. Immunfluorescence images show that at low concentrations IC261 leads to centrosome amplification causing multipolar mitosis. Our data are consistent with a role for CK1δ and CK1ε isoforms in regulating key aspects of cell division, possibly through the regulation of centrosome or spindle function during mitosis. *Oncogene* (2000) **19,** 5303–5313.

Keywords: casein kinase 1; mitotic checkpoint; chromosome segregation; centrosome amplification; micronucleation

Introduction

Casein kinase 1 (CK1) contain a family of highly related, constitutively active serine/threonine protein kinases (reviewed in Christenson *et al*., 1997; Gross and Anderson, 1998). CK1 is ubiquitously expressed in eukaryotes. Mammalian family members comprise three alternatively spliced α isoforms as well as β, γ1, γ2, γ3, δ and ε isoforms (Fish *et al*., 1995; Graves *et al*., 1993; Rowles *et al*., 1991; Zhai *et al*., 1995). These isoforms share a high degree of similarity within their protein kinase domains. For example CK1δ and CK1ε are 98% identical in this region (Fish *et al*., 1995; Graves *et al*., 1993), but show considerable variation in the presence, length and primary structure of the C-terminal non-catalytic domain (Christenson *et al*., 1997). These variable C-terminal domains are responsible for substrate specificity of the different isoforms (Cegielska *et al*., 1998; Graves and Roach, 1995), and are involved in the regulation of the interaction with other proteins, and/or subcellular structures. Phosphorylation (Cegielska *et al*., 1998) and perhaps dimerization in the case of CK1δ (Longenecker *et al*., 1998) are additional mechanisms that regulate CK1 activity, specificity, and subcellular localization. The list of known substrates of the CK1 family is still increasing, and so far includes cytoskeletal proteins such as spectrin, troponin, myosin and tau (Simkowski and Tao, 1980; Singh *et al*., 1983, 1995), and transcriptional components such as RNA polymerases I and II, SV40 T antigen and CREM (Dahmus, 1981; de Groot *et al*., 1993; Grässer *et al*., 1988).

Both, CK1δ and CK1ε, have been reported to phosphorylate p53 *in vitro* and in cultured cells (Knippschild *et al*., 1997; Milne *et al*., 1992b). The residues phosphorylated by these isoforms, and by high levels of CK1α *in vitro*, are serines 4, 6 and 9 in murine p53 (Higashimoto *et al*., 2000; Knippschild *et al*., 1997; Milne *et al*., 1992a), and threonine 18 in human p53 (Dumaz *et al*., 1999; Sakaguchi *et al*., 2000). However, the effect of phosphorylation by these two kinases on p53 activity is not yet known, neither is it clear what the biological significance of the p53-CK1 interaction might be.

Real advances in our understanding of the biology of CK1 have been provided by a number of genetic analyses in yeasts. The *S. cerevisiae hrr25* gene encodes a homologue of mammalian CK1δ and CK1ε; *hrr25* mutants show sensitivity to DNA damage and are defective in nuclear segregation and meiotic division (Hoekstra *et al*., 1991). CK1δ and CK1ε, but not CK1α, can complement *hrr25* mutations in yeast, suggesting that the mammalian and yeast proteins may have functional similarity (Christenson *et al*., 1997; Graves *et al*., 1993). In *S. pombe* the homologous *hhp1* and *hhp2* genes may play similar roles to *hrr25* and deletion of these genes generates large multinucleated cells (Dhillon and Hoekstra, 1994).

Additional evidence links CK1 function with chromosomal maintenance. For example, DMCK1 (the homologue of CK1α in *D. melanogaster*), is activated following DNA damage and relocates to the nucleus (Santos *et al*., 1996), while mammalian CK1α is located at the mitotic spindle and the

*Correspondence: U Knippschild
[3]Current address: Department of Anatomy and Physiology, Wellcome Trust Building, University of Dundee, Dundee DD1 4HN, UK
Received 9 September 2000; revised 20 September 2000; accepted 21 September 2000

centrosomes in both mouse fibroblasts and oocytes (Brockman *et al*., 1992; Gross *et al*., 1997). Recently we showed that CK1δ is recruited to the mitotic spindle and the centrosomes following treatment with etoposide or γ-irradiation in rodent cells (Behrend *et al*., 2000). The radiation treatment prior to mitosis frequently leads to centrosome overduplication and multipolar spindle (Behrend *et al*., 2000; Sato *et al*., 2000), morphologies that are known to activate the mitotic checkpoint. Thereby, the recruitment of CK1δ to the spindle/centrosome in aberrant mitotic cells may be interconnected with a mitotic checkpoint signal.

This view is also supported by the close link of CK1δ to the tumor suppressor protein p53 (s. above). Next to its role in DNA-damage checkpoint control (Agarwal *et al*., 1995; Kastan *et al*., 1991) p53 also has been shown to participate in the response to aberrant mitosis (Cross *et al*., 1995; Lanni and Jacks, 1998; Minn *et al*., 1996; Wahl *et al*., 1996b). It is now generally believed that p53 is not a key component of the spindle assembly checkpoint itself but prevents transition of abnormal postmitotic cells from G1 to S phase (Kahn *et al*., 1998; Lanni and Jacks, 1998). However, the nature of the signaling mechanism(s) through which p53 senses the damage of cells treated with spindle drugs is not known.

In the present paper we describe the effect of an ATP-competitive inhibitor IC261 with differential activities among CK1 isoforms (Mashhoon *et al*., 2000) in a wild-type or mutant p53 containing tumor cell line (MethAtsp53 cells) as well as in p53 wild-type (+/+ MEFs), p53 plus-minus (+/− MEFs) and p53-null mouse embryo fibroblasts (−/− MEFs). After p53-independent mitotic delay IC261 induces a p53-dependent G1 arrest. In cells lacking active p53 we observed endoreduplication, resulting in an 8N DNA content, coupled with morphological changes characterized by large flattened cells predominantly containing micronuclei. Immunofluorescence microscopy of IC261-treated mitotic cells showed centrosome overduplication and multipolar mitosis. We conclude that CK1δ/ε activity is indispensable for an ordered mitotic progression probably by regulating centrosome and/or spindle functions.

Results

Effects of IC261 on cell cycle distribution and cell survival in murine tumor cell lines

In order to determine whether CK1δ and CK1ε activity is required for normal cell cycle progression we have made use of the novel, well-characterized inhibitor IC261. IC261 (Icos Corp., USA) selectively inhibits CK1 compared to other protein kinases by an ATP-competitive mechanism. Moreover, IC261 shows an order of magnitude higher selectivity for CK1δ and CK1ε over other CK1 isoforms. The basis of CK1 specificity has been established at 2.8 A resolution by X-ray crystallography (Mashhoon *et al*., 2000).

The effects of IC261 in the low micromolar range on cell cycle distribution of primary mouse embryo fibroblasts (MEFs) (2. passage) with different p53 status (p53+/+, p53+/− and p53−/−) were measured by flow cytometry (Figure 1a). The cell cycle distribution profiles indicate that, 12 h after exposure to the drug, the MEFs arrested with a 4 N DNA content, independently of the p53 status. At subsequent timepoints, the profiles show distinct differences depending on the p53 status of the cells. p53+/+ cells predominantly remain in the 4 N arrest with only 22% of the cells with a higher DNA content while p53+/− (30%) and in particular p53−/− cells (57.5%) developed a larger 8 N population. The increase of a 8 N population in −/− MEFs was accompanied by a strong decrease in the proportion of cells with a 4 N content to 21.6% after 48 h.

In all investigated MEFs the treatment with IC261 increases the incidence of a sub-G1 fraction in the flow cytometry profiles indicating a possible apoptotic effect of the kinase inhibitor IC261. To evaluate the cytotoxic effect of IC261 on cultured cells we performed a combined PI-AnnexinV binding procedure (Vermes *et al*., 1995). MEFs were incubated with 1 μM IC261 and were assayed for a necrotic (PI+/FITC+) or an apoptotic (PI−/FITC+) subfraction (Figure 1b). In the untreated controls we found almost exclusively viable cells (PI−/FITC−); the amount of apoptotic cells in MEFs of all three genotypes were below 4%. The application of IC261 increases the amount of apoptotic cells after 3 days up to 40% in −/− MEFs whereas only 23.4% of +/− MEFs and only 15.2% of +/+ MEFs show AnnexinV binding. The quantity of non-binding PI 'stained cells' indicating a possible necrotic effect were negligible in all performed experiments. The diagram following the progression of apoptosis shows an increasing subpopulation of apotic cells in all three MEFs up to the fourth day of IC261 treatment but with a slightly higher amount in +/− MEFs and markedly higher amount in −/− MEFs compared to +/+ MEFs.

Taken together, these data are consistent with IC261 leading to a p53-dependent arrest of the cells with a DNA content of 4 N. In cells with a relaxed (p53+/− cells) or without p53 response (p53−/− cells) IC261 induced an increase in ploidy compared to p53+/+ cells. The higher DNA content is accompanied with a rise in the number of cells commited to the apoptotic pathway. Therefore, the p53-dependent arrest may protect cells from apoptosis in the presence of IC261.

IC261, like nocodazole (NOC), leads to wt p53-dependent postmitotic arrest

Most drugs that induce an increase of DNA content belong to the group of spindle inhibitors. We therefore compared the effects of IC261 on cell cycle progression with that of the microtubule inhibitor nocodazole (NOC). We tested the effects of IC261 and NOC on MethAtsp53 cells, a cell line which ectopically expresses the 'valine 135' temperature-sensitive p53 mutant. At 39°C tsp53 is in a mutant conformation, but wild-type functions can be restored by shifting the cells from growth at 39°C to 30°C where a significant proportion of the p53 protein is in the wild-type conformation (Otto and Deppert, 1993). The particular advantage of this cell line is that cells continue to grow at the permissive temperature, owing to high levels of MDM2 (Knippschild *et al*., 1995; Otto and Deppert, 1993).

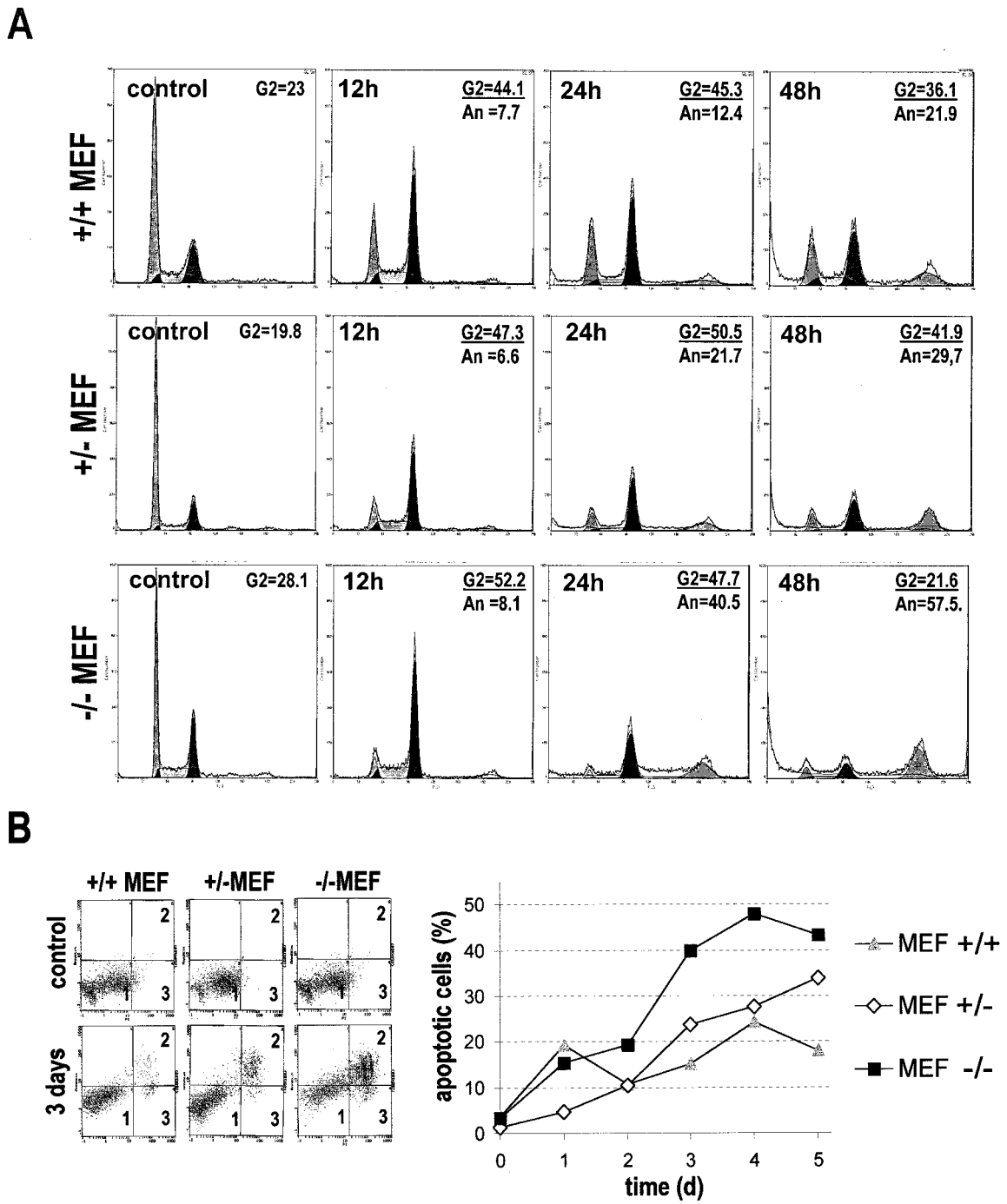

Figure 1 Analysis of the effects of the CK1δ/ε-specific inhibitor IC261 on cell cycle distribution and survival of MEFs. Cultures of MEFs (passage no 2) of different genotypes (p53+/+, p53+/−, p53−/−) were treated with the CK1δ/ε-specific kinase inhibitor IC261 in the low micromolar range (1 μM). (**a**) At the specified time points cells were trypsinized, washed in PBS, fixed in 70% ethanol and stained with PI (Material and methods). Flow cytometry of cells was performed on a Coulter Epics XL-MCL; calculation of cell cycle stages was done using the cell cycle analysis program WinCycle for Windows. (**b**) For measurement of apoptotic or necrotic effects of IC261, MEF cells were collected after different time points following IC261 treatment. PBS-washed cells were incubated with FITC-coupled Annexin V to detect apoptosis and afterwards stained with PI to detect necrotic cells (Material and methods). The two-parametric flow cytometry displays distinct populations of viable (PI−/FITC−(1)) and apoptotic (PI−/FITC+(2)) but only few necrotic (PI+/FITC+(3)) cells. Quantification of the subpopulations was done using the program System II, 3.0 version (Coulter)

Flow cytometry analysis of PI-stained cells showed that, both IC261 and NOC treatment gave rise to an increase in the cellular DNA content in MethAtsp53 cells when grown at 39°C (Figure 2). Sixteen hours after drug exposure, 55% of the cells treated with 0.6 μM IC261 and 60% of cells treated with 0.4 μM NOC had an aneuploid DNA content (An) greater than 4 N. At 24 h and 48 h post-treatment, up to 90% of the cells treated with IC261 and 75% of NOC treated cells had exactly doubled their DNA to an 8 N content. As expected, we received the same result with the parental MethA cells (data not shown).

In MethAtsp53 cells shifted to 30°C (Figure 2b) drug treatment increased the 4 N population to 43% after 72 h IC261 treatment, respectively to 32% in the presence of 0.4 μM NOC. In comparison, shifting cells to 30°C for

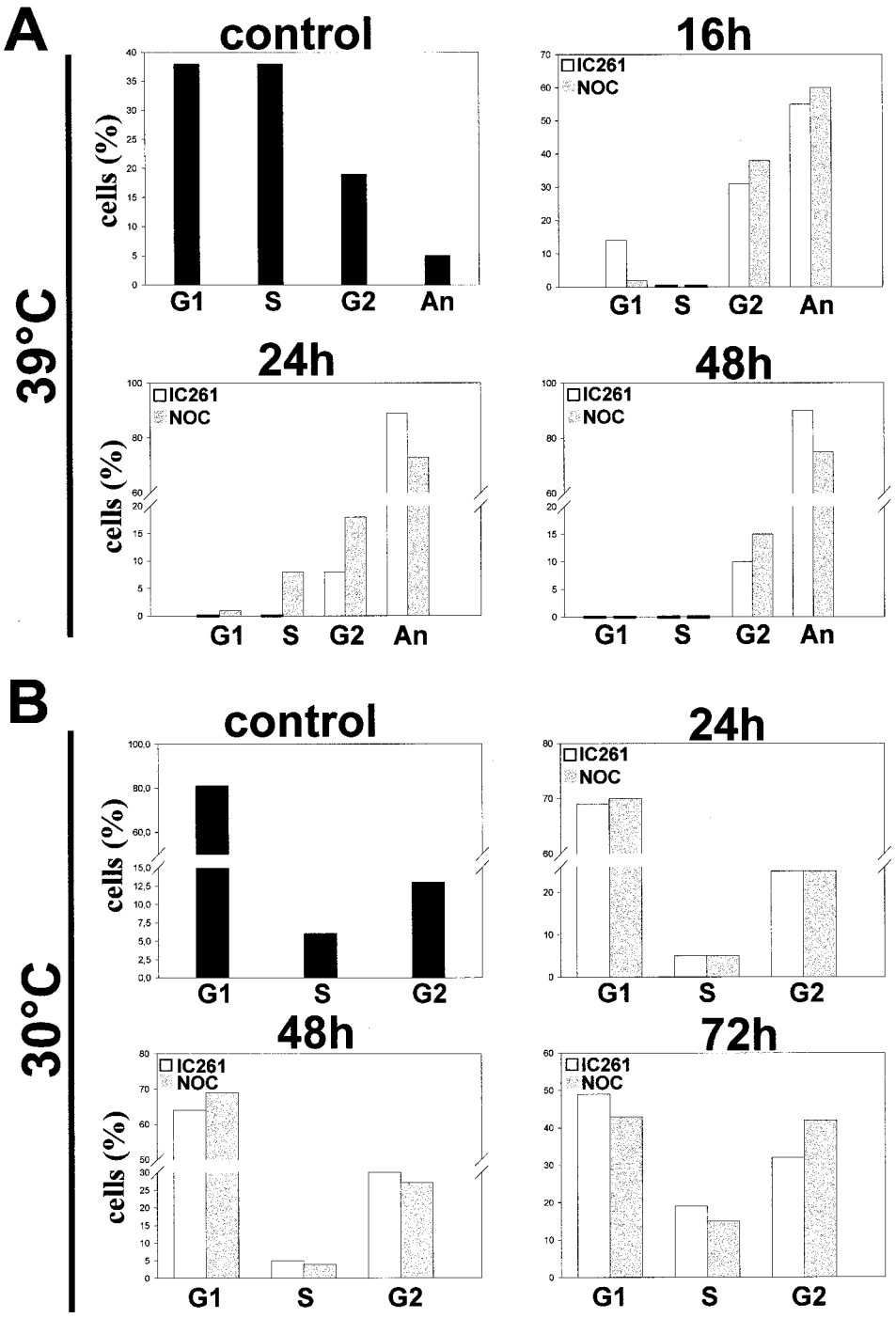

Figure 2 Comparison of IC261 and NOC induced effects on cell cycle distribution in MethAtsp53 cells at the non-permissive (39°C) (**a**) and permissive temperature (30°C) (**b**). MethAtsp531 cells were treated with 0.6 μM of the CK1δ/ε-specific kinase inhibitor IC261 or alternatively with 0.4 μM of the microtubule disrupting drug NOC for the indicated time points. Cells were grown at the non-permissive temperature or were shifted to the permissive temperature 16 h before drug treatment. Ethanol fixed, PI-stained cells (Material and methods) were analysed by flow cytometry on a Coulter Epics XL-MCL and subpopulations were calculated with the cell cycle analysis programm WinCycle. The diagrams show the percentage of cells in the indicated cell cycle stages

same time periods without drug treatment only leads to a slight increase of cells with a 4 N DNA content (data not shown). Taken together, the data indicate that IC261 can produce effects on cell cycle progression that are indistinguishable from an established spindle poison and are dependent on the p53 status of the cells.

The increase of ploidy by inhibition of spindle assembly is characteristic of many cancer cell lines (Roberts *et al*., 1990). In these cells the loss of spindle checkpoint control leads to the uncoupling of cytokinesis and replication resulting in 8 N or even 16 N DNA contents. Most often the increase in ploidy is accompanied by the enlargement of the cells and the development of micronuclei (Fujikawa-Yamamoto *et al*., 1997). To investigate the possibility that the kinase inhibitor leads to similar postmitotic effects, we investigated the nuclear morphology of MethAtsp53 cells using combined brightfield-fluorescence images of

DAPI-stained cells (Figure 3a). Whereas untreated MethAtsp53 cells grown at 39°C show predominantly a small rounded shape, cells treated with IC261 or NOC were significantly enlarged. Additionally, the fluorescence staining of the chromatin with DAPI displays micronucleation after both treatments. In contrast, in cells grown at 30°C neither NOC nor IC261 induces micronucleation or other microscopically detectable changes compared to control cells (data not shown). Considering the generation of micronuclei over the time (Figure 3b), it is obvious that NOC induces micronucleation to a greater extent (up to 88%) than the kinase inhibitor IC261 (up to 37%), at least at the used concentration of 0.6 μM. In MethAtsp53 cells grown at 30°C both inhibitors had no effect on the amount of micronucleated cells. Thus, with respect to nuclear morphology and cell cycle distribution, the response of the MethAtsp53 cells to IC261 showed striking similarity to the response to NOC.

IC261 treatment results in a p53-independent transient mitotic arrest

The similarities in the response to the CK1δ/ε specific inhibitor IC261 and to the spindle drug NOC suggest that CK1δ/ε activity is required for normal mitotic passage. Spindle drugs interfere with mitotic progression by preventing the assembly of the spindle apparatus leading to a significantly prolonged mitosis (Kahn *et al*., 1998; Lanni and Jacks, 1998). In order to determine changes in mitotic kinetics as a result of inhibition of CK1δ/ε we made use of the monoclonal antibody MPM-2, which recognizes a conserved epitope shared by mitotic phosphoproteins (Davis *et al*., 1983). For this purpose MEFs with different p53 backgrounds (p53+/+, p53+/− and p53−/−) were treated with 1 μM IC261 and analysed by two-parametric flow cytometry after different time points. Simultaneous staining of MPM-2 with a FITC-coupled IgG and DNA by PI permitted the detection of a distinct population of mitotic cells (Figure 4). Exposure to IC261 led to an immediate increase of a mitotic subpopulation after 6 and 12 h independently of the genetic background of different MEFs. As shown in the diagram in Figure 4, all three cultures displayed a peak of MPM-2 reactivity after 12 h but MPM-2 signal decreases after 24 and 48 h. The temporary increase of MPM-2 reactivity has to be explained by a transient arrest in mitosis prior to metaphase-anaphase transition at which dephosphorylation of MPM-2 antigens takes place (Vandre and Borisy, 1989). The similarities in changes of mitotic kinetics in MEFs with and without p53 indicate that the IC261-induced mitotic delay is independent of the p53 status of the cells.

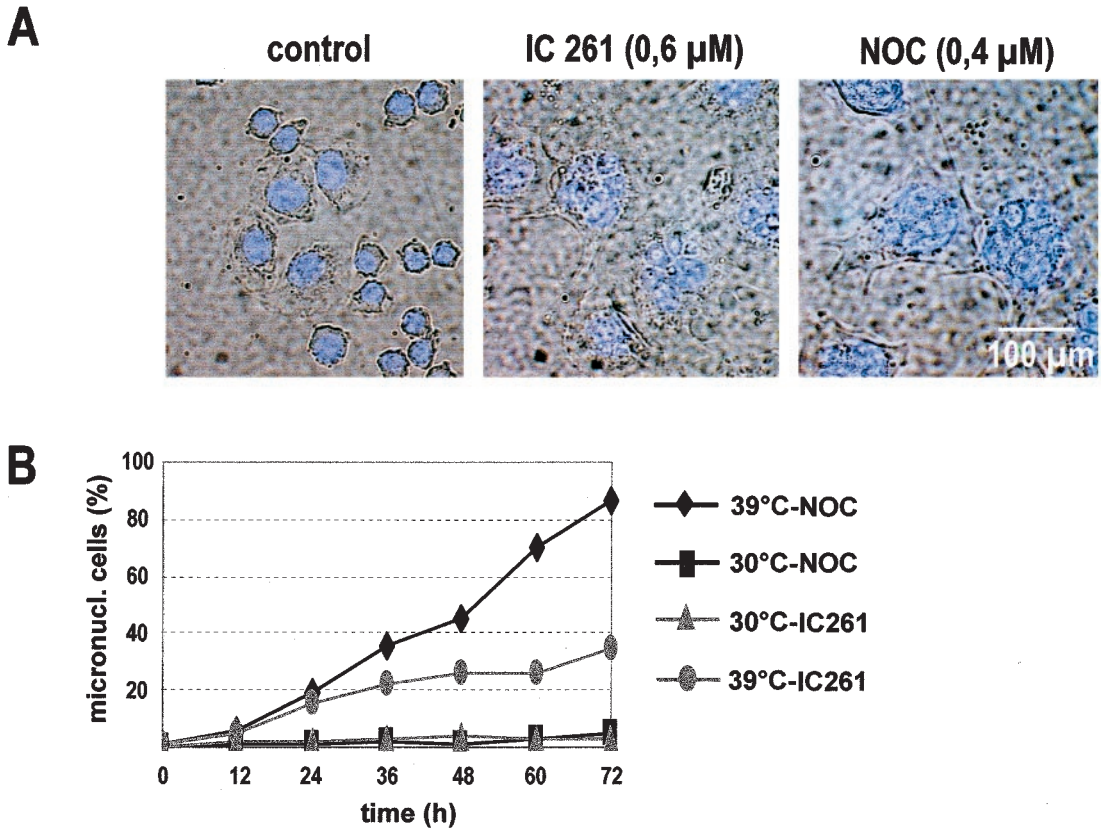

Figure 3 Micronucleation in IC261 and NOC treated cells in the absence of active p53. (**a**) MethAtsp53 were grown at the non-permissive temperature at 39°C. Cells treated either with the kinase inhibitor IC261 or the spindle inhibitor NOC for 48 h were stained with DAPI to visualize the DNA and compared with untreated cells. Merged images of brightfield and blue fluorescence show micronucleation in the treated but not in the untreated cells. (**b**) To quantify the effects of NOC and IC261 on micronucleation at the concentrations indicated in (**a**), we counted micronucleated versus non-micronucleated MethAtsp531 cells at both, the permissive (■NOC/▲IC261) and non-permissive temperature (◆NOC/●IC261)

G1-like status of postmitotic arrested, wt p53 containing cells

Consistent with the published model for drugs that trigger the spindle checkpoint (Di Leonardo *et al*., 1997; Minn *et al*., 1996), IC261 treated cells expressing functional p53 show a mitotic delay and finally arrest with a 4 N DNA content at the G1/S boundary. To confirm that IC261 treated cells with active p53 arrest in G1, we investigated the cyclin A status of IC261-arrested MethAtsp53 cells, shifted to the permissive growth temperature of 30°C.

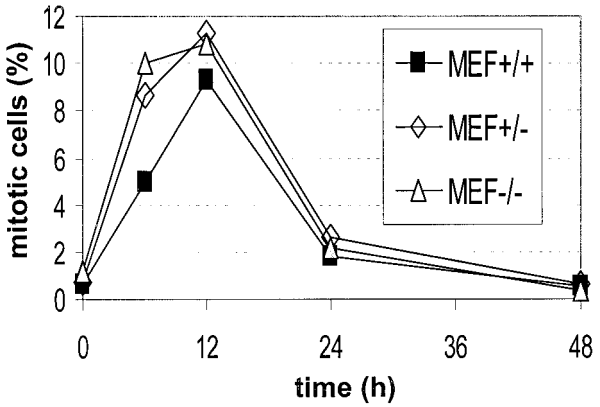

Figure 4 Treatment with IC261 results in a transient mitotic arrest of p53+/+ (■), p53+/− (◇) and p53−/− MEFs (▲). MEFs were fixed in 70% ethanol and stained for MPM2 and PI (Material and methods). In a two-parametric flow cytometry diagram a MPM-2 positive, 4N containing subpopulation were detected. The statistical analysis revealed a transitory increase of the mitotic population after IC261 treatment independent of the genotype of MEFs

Cyclin A begins to accumulate at the G1/S transition and persists through S and G2 phase. Cyclin A-associated kinase activity is required for S phase, completion of S phase and entry into mitosis, but has to be degraded to exit from mitosis (Lehner and O'Farrell, 1989; Walker and Maller, 1991). Simultaneous staining of cyclin A-FITC and DNA with PI of untreated MethAtsp53 cells maintained at 30°C revealed, as expected, that cyclin A levels increased in 4 N cells (G2 phase) in comparison to 2 N cells (G1 phase) (Figure 5a). In contrast, 8 h after IC261 treatment, we observed a remarkable decrease of cyclin A reactivity in 4 N containing cells. At later timepoints the cyclin A antigen status of 4 N containing cells nearly matches that of G1 cells. Therefore, our data support the hypothesis that cells expressing p53 in its wild-type conformation, although containing a double set of chromosomes, arrest IC261-dependent in the postmitotic G1 phase. To confirm this G1-like status of MethAtsp53 cells maintained at 30°C we determined the phosphorylation status of the retinoblastoma protein (Rb). The phosphorylation of Rb is a key event in transition of cells at the G1/S boundary (Thomas *et al*., 1991). Immunoblot analysis of lysates from MethAtsp53 cells shifted to 30°C show an increase of the amount of hypophosphorylated Rb 48 h (lane a) and 72 h (lane b) after treatment with IC261 (Figure 5b) compared to Rb from untreated cells (lane c). The reduced phosphorylation of Rb and the Cyclin A-negative status of IC261-arrested functional active tsp53 containing cells can only be explained by IC261 inducing a postmitotic G1 arrest. As expected, in cells grown at 39°C IC261 treatment (lanes d, e) did not change the amount of hypophosphorylated Rb in comparison to the control (lane f) indicating

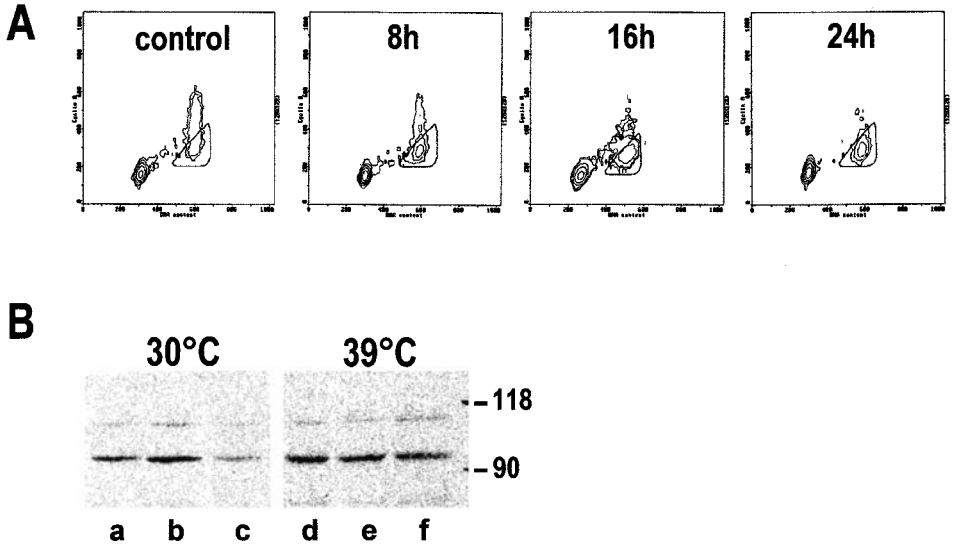

Figure 5 MethAtsp53 cells kept at the permissive temperature (30°C) and expressing p53 in wt conformation arrest in G1 after treatment with IC261. (**a**) IC261 treated (8, 16, 24 h) and untreated (control) MethAtsp53 cells were maintained at 30°C, fixed in 70% ethanol and stained for cyclin A using a rabbit polyclonal antibody against cyclin A followed by incubation with a FITC-coupled anti-rabbit IgG. In addition, to simultaneously determine the cell cycle stages, cells were stained with PI. The two-parametric flow cytometric analysis shows an increase in cyclin A-positive, 4N containing cells by time. (**b**) To determine the phosphorylation status of Rb, lysates from untreated (c, f) and IC261 treated (1 μM IC261 for 48 h and 72 h) (a/d, b/e) MethAtsp53 cells grown at the permissive (a–c) and non permissive temperature (d–f) were subjected to SDS–PAGE. Proteins were blotted onto nitrocellulose membranes and probed with a monoclonal anti-Rb IgG. Immunocomplexes were visualized by a HRP-coupled anti-mouse IgG and subsequent chemiluminescence detection

the loss of checkpoint function of p53 in its mutant conformation.

IC261 interferes with ordered mitosis by inducing centrosome amplification and multipolar mitosis

To follow up the idea that the mitotic delay of IC261-treated cells is a result of interference with ordered mitosis we analysed mitotic cells 8 to 12 h after IC261 treatment. We collected mitotic shake off cells from the media and prepared suspended cells by cytospin. Mitotic spindles and centrosomes were analysed by immunofluorescence microscopy using antibodies against β-tubulin and γ-tubulin, respectively. The cellular chromatin was visualized by DAPI-staining.

The images presented in Figure 6a,b show untreated C57MG cells. The metaphase cell in Figure 6a represents an ordered mitotic architecture with all chromosomes aligned at the metaphase plate displaying two spindle poles. In addition to metaphase cells we detected cells in anaphase, telophase and cytokinesis (Figure 6b).

The treatment of cultures with different concentrations of NOC interferes with an ordered mitotic architecture (Figure 6c,d). Using 0.4 μM NOC, a concentration normally used for induction of the spindle checkpoint, absolutely suppresses the assembly of mitotic spindles (Figure 6c). Additionally, instead of having only two centrosomes the NOC-treated cells exhibited multiple γ-tubulin positive structures. In cells treated with lower concentrations of 0.1 μM NOC a small amount of tubulin is assembled in microtubule structures, but without showing a true spindle architecture (Figure 6d). Instead, short radial orientated microtubule assemblies surround γ-tubulin positive spots. At this lower concentration only the elongation of spindles, but not the nucleation of spindles from the γ-tubulin-positive structures (possibly centrosomes), seems be inhibited.

In contrast to NOC-treated cells, in cells treated with 0.6 μM IC261 we observed assembled spindles (Figure 6e–h). Analysis of mitotic cells revealed three different groups of cells. In the first group represented by the cells shown in Figure 6e,f we found bipolar mitosis but frequently with failures of the spindle structure. The most prominent modification is the ring-shaped dispersion of pericentriolar material. In the second group we found multipolar spindle and a distribution of centrosomal structures in the entire cell (Figure 6g). Also, in a minority of cells, we observed a regular mitotic architecture (Figure 6h): a bipolar undisturbed spindle with two spindle poles and metaphase chromosomes regularly aligned at the metaphase plate. However, in contrast to the situation in non-treated cells, we could never detect mitotic cells treated with IC261 in anaphase or telophase arguing for a metaphase-arrest of the cells. The immunofluorescence images demonstrate that the IC261-induced delay in mitosis is often accompanied by alterations in mitotic architecture but generally without interference with spindle assembly.

While IC261 has strong effects on spindle architecture immunofluorescence microscopy of interphase cells revealed no detectable effect of IC261 on microtubule structure at concentrations specific for inhibition of CK1δ/ε (data not shown). Therefore, at the used concentration, the morphological effects of IC261 seems to be restricted to mitosis.

Discussion

The data presented in this paper show that IC261, a specific inhibitor of the delta and epsilon isoforms of

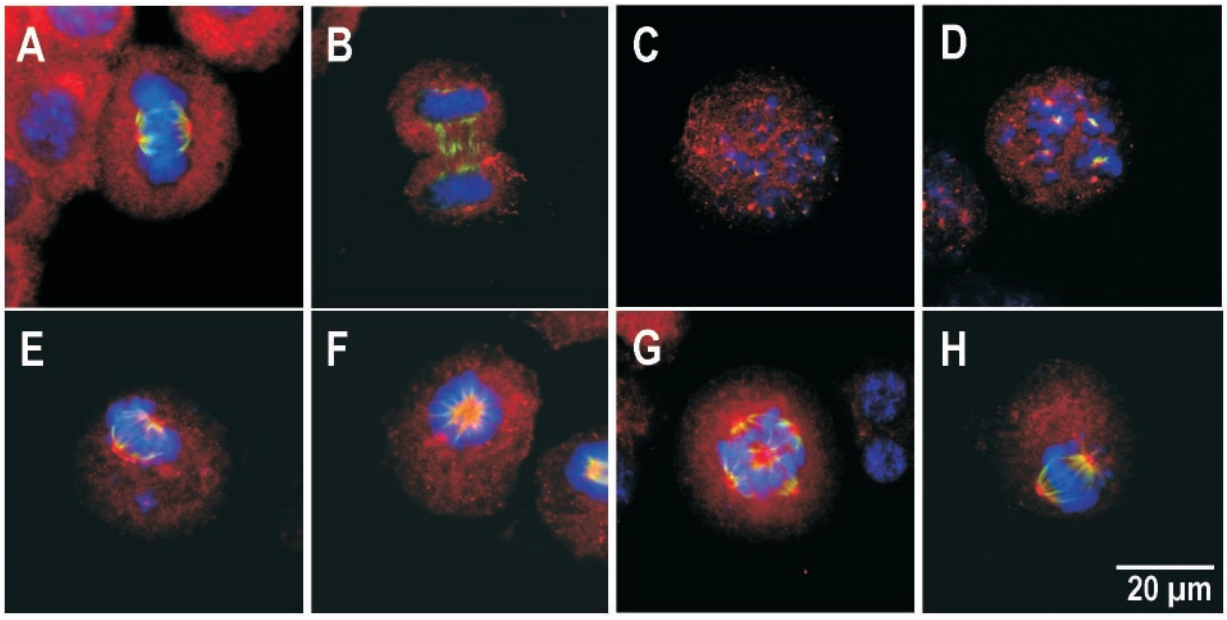

Figure 6 IC261 and NOC induce differential defects in the architecture of the mitotic apparatus. Untreated C57MG cells (**a**, **b**), cells treated with 0.4 μM (**c**) or 0.1 μM NOC (**d**) for 12 h and cells treated with 0.6 μM IC261 for 12 h (**e**–**h**), respectively, were prepared for immunofluorescence staining by cytospin from the media (mitotic shake off cells). Cells were stained using monoclonal anti-β-tubulin followed by FITC-coupled anti-mouse IgG and polyclonal anti-γ-tubulin followed by rhodamine-coupled anti-rabbit IgG, respectively. Accordingly, the spindles are visualized in green and the centrosomes are seen in red by indirect immunofluorescence staining. The DNA was stained in blue by DAPI

protein kinase CK1 has profound effects on the progression of early passage embryo fibroblasts and of MethAtsp53, a cultured line expressing a temperature-sensitive p53 protein. Specifically, IC261 arrests cells expressing functional p53 in the postmitotic G1 phase, whereas cells which lack functional p53 function override the checkpoint control and undergo endoreduplication, most of them developing micronuclei. Several studies have shown that classical microtubule-disrupting or -stabilizing agents including NOC, colcemid and paclitaxel show precisely these phenotypes on p53-competent and p53-null cells (Cross *et al*., 1995; Di Leonardo *et al*., 1997; Gualberto *et al*., 1998; Lanni and Jacks, 1998; Minn *et al*., 1996; Notterman *et al*., 1998; Sablina *et al*., 1998; Wahl *et al*., 1996a). Our own analyses using NOC (Figures 2 and 3) are consistent with these observations. Moreover, exposing either p53-competent or p53-defective cells to an inhibitor of CK1δ/ε produces effects which are strikingly similar to those of NOC interfering with ordered mitotic progression. These data are consistent with the idea that CK1δ/ε plays an essential role in maintaining the integrity of cell cycle progression by controlling key functions in chromosome segregation.

The role of p53 in the control of the mitotic checkpoint has been the subject of discussion over the last few years. While Cross *et al*. (1995) suggested a direct involvement of p53 in the mouse spindle checkpoint, more recent analyses have disproved the direct association of p53 with spindle assembly control. For example, mutants that lack components of the spindle assembly checkpoint, such as the BUB or MAD gene products first identified in budding yeasts (Dobles *et al*., 2000), fail to accurately segregate chromosomes. In contrast p53-negative cells are still able to traverse mitosis. Moreover, the kinetics of mitotic progression in the presence of spindle inhibitors are not influenced by the p53 status of the cells (Lanni and Jacks, 1998).

The current perception of the role played by p53 in responding to spindle disruption is that p53 acts in a postmitotic manner preventing damaged cells from proceeding through S phase. The data obtained from the treatment of cells with IC261 are consistent with results disproving a direct involvement of p53 in mitotic checkpoint. The quantification of mitotic cells by measuring the MPM-2-status in IC261 treated p53+/+, p53+/− and p53−/− MEFs showed that the kinetics of delayed mitosis in these cells are approximately the same. Therefore, inhibition of CK1δ/ε activity prolongs mitosis in a p53-independent manner. These results are consistent with a MPM-2-based flow cytometric assay of Khan and Wahl (1998) showing same results with NOC. The resemblance between IC261 and NOC mediated early (mitotic delay) and late effects (postmitotic G1 arrest, respectively endoreduplication) in cells with and without a mitotic checkpoint control strongly suggests that IC261 itself triggers the mitotic checkpoint.

Drugs that interfere with an ordered chromosome segregation, and therefore with cytokinesis, induces apoptosis (Woods *et al*., 1995). In this study, we present that IC261 like spindle drugs induces apoptosis in both, cells with and without checkpoint activity of p53. Treatment of p53 wild-type MEFs with IC261 immediately after 24 h induces apoptosis rates near 20% that stay the same over following days. In p53-null MEFs apoptosis rates constantly rises up to the fourth day to approximately 50%. Interestingly, the extend of apoptosis at later timepoints rises in correlation with the loss of checkpoint function in the order +/+, +/−, −/− MEFs. Therefore, this later cell death (3–5 days) seems to be reasoned in the progression beyond the G1/S postmitotic checkpoint in p53-null cells. The pronounced p53-independent apoptotic effect should turn attention on a possible therapeutic applicability of IC261 as a large fraction of human cancers are mutated in the p53 gene.

While the effects of chemotherapeutics which interfere with spindle assembly (classical spindle poisons) or stabilize microtubules (taxoids) are partly understood, the nature of interference of IC261 with mitotic progression was unknown and was therefore addressed. The investigation of the mitotic architecture of cells treated with submicromolar concentrations of IC261 or NOC respectively revealed a characteristic distinction. In contrast to NOC-treated cells, we found that the assembly of spindle microtubules stained by anti-β-tubulin antibodies is not generally inhibited by IC261. Nevertheless, unlike untreated mitotic cells, most IC261-treated cells showed a drastic amplification of spindle poles. In addition, DAPI-staining of these cells showed fully condensed but randomly spread chromosomes; a phenotype we also found in NOC arrested cells. IC261, therefore, resembles spindle poisons that inhibit the correct positioning of chromosomes in metaphase. While the condensation of chromosomes is dispensable for an intact spindle apparatus the movement of chromosomes towards the metaphase plate is a microtubule dependent phenomenon. This supports the argument that IC261 interferes with spindle function probably by modulating the dynamics of the spindle. As we found no influence of IC261 on cell shape or cytoskeleton in interphase cells and, in addition, IC261 had no effects on resting cells, we conclude that IC261 selectively interferes with microtubule dynamics during mitosis.

The effects of IC261 on cell cycle progression and apoptosis can be attributed to targeting of the spindle during an early mitotic stage. The question then arises as to whether CK1δ/ε is indeed the major target of IC261 and consequently what is the role of CK1δ/ε during mitosis? So far the precise mechanisms that regulate the rapid process of spindle assembly are unclear. In recent years a growing number of studies have underscored the important role of tubulin associated proteins in spindle dynamics, especially those of microtubule associated proteins (MAPs), catastrophe factors (reviewed in Andersen, 2000) and motor proteins (reviewed in Mountain and Compton, 2000). The comprehensive effects of IC261 on spindle architecture before cells reach the metaphase border point to IC261 directly influencing spindle dynamics. Indeed, our and the work of other groups implicate a direct connection of the CK1 family to spindle functions. As seen from immunofluorescence and co-immunprecipitation experiments, CK1δ specifically associates with the spindle and the centrosomes in cells with irregular mitosis (Behrend *et al*., 2000). The close vicinity to microtubules is also expressed in the substrate specificity of CK1δ. CK1δ is known to phosphorylate tubulins, the microtubule associated

proteins tau and MAP4 and stathmin (Behrend *et al*., 2000; Kuret *et al*., 1997; Singh *et al*., 1995). Indeed we found, that inhibition of CK1δ/ε by IC261 changes the *in vivo* phosphorylation pattern of some of the mentioned *in vitro* substrates (Stöter *et al*., paper in preparation). A number of accessory proteins capable of stabilizing or destabilizing microtubule polymers are modified and regulated by cell cycle-dependent phosphorylation. Through this regulation, microtubule dynamics are modified to generate rapid microtubule turnover during mitosis (reviewed in Cassimeris, 1999). We suppose that IC261 mediated intervention with spindle functions may be the result of reduced phosphorylation of spindle accessory proteins and, therefore, influencing the balance between stabilizers and destabilizers.

Recently, CK1 has been connected to another group of tubulin associated proteins, the motor proteins. It has been shown that CK1 from *Chlamydomonas* interacts with the intermediate chain of dynein in the axonem of the flagella (Yang and Sale, 2000). Because the inhibition of phosphorylation of dynein by specific inhibitors of CK1 rescues a mutant with reduced flagella rotation authors stated CK1 as a negative regulator of flagellar movement. Dynein and members of the dynein-associated dynactin complex have been implicated in the positioning of the mitotic spindle *in vivo* (reviewed in Busson *et al*., 1998) or in the formation of the spindle in cell extracts (Palazzo *et al*., 1999; Walczak *et al*., 1998). If the results connecting CK1 to dynein functions could be confirmed in mammalians this would raise dynein to a possible target for IC261. The interference with dynein-mediated movements would explain the observed disturbance of the spindle apparatus. Some of these kinesin-related motor proteins are located to the spindle and/or centrosomes and display functions in the spindle organisation, the centrosome separation and positioning (Agarwal *et al*., 1998; Boleti *et al*., 1996; Gaglio *et al*., 1996; Sharp *et al*., 1999). For example ncd is located to centrosomal microtubules and spindle fibers and seems to be critical for poleward movement of chromosomes in mitosis. Interestingly, mutants of the *Drosophila* ncd microtubule motor protein cause centrosome splitting and loss of centrosomes from spindle pole (Endow *et al*., 1994), much the same defects induced by IC261.

Taken together, we provide strong evidence that CK1δ and ε are key proteins in chromosome segregation as the specific inhibitor of both isoforms IC261 is intervening with mitosis and triggers p53-dependent mitotic checkpoint. We speculate here that the critical step in IC261 induced effects may be the interference with CK1δ/ε-specific phosphorylation of spindle component proteins. However, this hypothesis derived from cellular biology remains to be tested by making use of molecular genetics.

Materials and methods

Cell lines and culture medium

Primary mouse embryo fibroblast (MEF) cultures with different p53 background (p53 +/+, p53 +/− and p53 −/−) were prepared from mechanically dispersed 17-day-old Balb/c mouse embryos by digestion with 0.2% collagenase in phosphate buffered saline (PBS). Primary MEF cultures and C57MG cells, a mouse mammary epithelial cell line (Vaidya *et al*., 1978), were grown in Dulbecco's modified Eagle's medium (DMEM) supplemented with 10% FCS at 37°C in a humidified 5% CO_2 atmosphere. MethA, a methylcholanthrene-transformed fibrosarcoma cell line (DeLeo *et al*., 1977) and MethAtsp53 cells, obtained after transfection of MethA tumour cells with a $tsp53^{val135}$ expressing vector (Otto and Deppert, 1993), were grown in DMEM supplemented with 5% FCS. MethAtsp53 cells were maintained at 39°C and in order to express tsp53 in wild-type conformation cells were shifted to 30°C.

Reagents and primary antibodies

The spindle inhibitor nocodazole (Sigma) and the kinase inhibitor IC261 (Icos Corp., Washington, USA) were solved in DMSO and stored at −20°C in 10 mM (nocodazole) and 25 mM (IC261) stock solutions.

For immunodetection we used polyclonal antibodies against γ-tubulin (Sigma) and cyclin A (Santa Cruz). Additionally, monoclonal antibodies against β-tubulin (Boehringer), MPM-2 (Upstate Biotechnology) and Rb (a gift from Irene Dornreiter, Hamburg) were used.

Immunofluorescence microscopy

Cells used for immunofluorescence staining were grown on coverslips or prepared by cytospin in a cytospin 3 centrifuge (Shandon) at 600 r.p.m. for 6 min. Cells were washed twice in PBS and fixed in 3% paraformaldehyde in PBS for 10 to 15 min at 37°C. Fixed cells were permeabilized in PBS containing 0.3% Triton-X-100 (Fluka) for 3 min at room temperature. Fixed cells were washed in PBS and blocked in PBS containing 0.2% gelatine for at least 1 h followed by an 1 h incubation with primary antibodies. Secondary antibodies were incubated for 30 min using FITC- or Rhodamine-labelled IgG (Dianova, Germany), respectively. DNA was visualized by DAPI staining (10 min; 0.1 μg/ml). Epifluorescence microscopy was performed using a Leica $63\times/1.4$ or $40\times/1.0$ oil immersion objective with a Leica DM-R microscope equipped with a high resolution digital camera system (Diagnostic Instruments, Intas, Germany).

Lysis, SDS–PAGE and Western immunoblotting

Cells were washed in ice-cold PBS, extracted for 30 min with a buffer containing 50 mM Tris-HCl, pH 8.0, 150 mM NaCl, 10% glycerol, 0.5% NP40, 5 mM DTT, 1 mM EDTA, 1 mM EGTA, 50 μM leupeptin and 30 μg/ml aprotinin, cleared by centrifugation for 30 min at $15\,000\times g$ and denatured in sodium dodecyl sulfate (SDS) containing sample buffer. After separation on SDS-polyacrylamide gels, proteins were transferred onto a nitrocellulose membrane (Hybond C super, Amersham Pharmacia Biotech.). The membranes were probed with specific antibodies. Immunocomplexes were detected using horse radish peroxidase conjugated with anti-mouse IgG (SAPU, GB, Scotland) followed by chemiluminescence detection (ECL, Amersham Pharmacia, Germany and Pierce, USA).

Flow cytometry

For flow cytometry analysis approximately 1×10^6 cells were collected from 9 cm culture dishes (Nunc) and fixed in ice-cold 70% ethanol following incubation for 15 min on ice and storage for at least 1 h at −20°C. To perform cell cycle analysis cells were washed in PBS and stained with a propidium iodide (PI)-solution containing 50 μg/ml PI (Sigma) and 10 μg/ml RNAse (Fluka) in PBS at 37°C for 30 min. For the staining of intracellular epitops ethanol fixed

cells were washed in wash solution (0.05% Triton-X-100 in PBS) and resuspended in 100 μl staining solution (0.2% Triton-X-100 and 2% FCS in PBS), supplemented with 2.5 μg/ml of the indicated antibody and incubated for 2 h at 4°C. Cells were then washed in wash solution and resuspended in staining solution with FITC-conjugated anti-mouse or anti-rabbit antibodies (Dianova, Germany) followed by incubation for 1 h at 4°C. Epitope stained cells were subsequently stained with PI-solution.

To evaluate apoptotic and/or necrotic effects of IC261 we used a method of Vermes *et al.* (1995), staining cells sequentially with FITC-coupled AnnexinV (Boehringer) and PI. This procedure permitted us to discriminate between viable cells (PI−/FITC−), apoptotic cells (PI−/FITC+) and necrotic cells (PI+/FITC+).

All indicated flow cytometric assays were made (with at least 10 000 cells) on a Coulter Epics XL-MCL flow cytometer. The quantification of cell populations was performed using the DOS software System II, 3.0 version, or for analysis of cell cycle distribution, the program MultiCycle for Windows.

Acknowledgments
We are grateful to our colleages Merl Hoekstra and Toni DeMaggio (ICOS Corporation, USA) who have kindly provided the CK1δ/ε specific inhibitor IC261. In addition, we thank Biny Mathew for technical assistance and Sonja Wolff for stimulating discussion. This work is supported by grants from the Deutsche Krebshilfe, Dr. Mildred Scheel Stiftung, to Uwe Knippschild (10-1285-Kn I) and from the Medical Research Council (UK) to David Meek. The Heinrich-Pette-Institut is financially supported by Freie und Hansestadt Hamburg and Bundesministerium für Gesundheit. The work is part of the PhD thesis of Lars Behrend, Fachbereich Biologie at the University of Hamburg.

References

Agarwal ML, Agarwal A, Taylor WR and Stark GR. (1995). *Proc. Natl. Acad. Sci. USA,* **92,** 8493–8497.
Agarwal ML, Taylor WR, Chernov MV, Chernova OB and Stark GR. (1998). *J. Biol. Chem.,* **273,** 1–4.
Andersen SS. (2000). *Trends Cell. Biol.,* **10,** 261–267.
Behrend L, Stoter M, Kurth M, Rutter G, Heukeshoven J, Deppert W and Knippschild U. (2000). *Eur. J. Cell. Biol.,* **79,** 240–251.
Boleti H, Karsenti E and Vernos I. (1996). *Cell,* **84,** 49–59.
Brockman JL, Gross SD, Sussman MR and Anderson RA. (1992). *Proc. Natl. Acad. Sci. USA,* **89,** 9454–9458.
Busson S, Dujardin D, Moreau A, Dompierre J and De Mey JR. (1998). *Curr. Biol.,* **8,** 541–544.
Cassimeris L. (1999). *Curr. Opin. Cell. Biol.,* **11,** 134–141.
Cegielska A, Gietzen KF, Rivers A and Virshup DM. (1998). *J. Biol. Chem.,* **273,** 1357–1364.
Christenson E, DeMaggio AJ and Hockstra MF. (1997). *Recent Results Cancer Res.,* **143,** 263–274.
Cross SM, Sanchez CA, Morgan CA, Schimke MK, Ramel S, Idzerda RL, Raskind WH and Reid BJ. (1995). *Science,* **267,** 1353–1356.
Dahmus ME. (1981). *J. Biol. Chem.,* **256,** 11239–11243.
Davis FM, Tsao TY, Fowler SK and Rao PN. (1983). *Proc. Natl. Acad. Sci. USA,* **80,** 2926–2930.
de Groot RP, den Hertog J, Vandenheede JR, Goris J and Sassone-Corsi P. (1993). *EMBO J.,* **12,** 3903–3911.
DeLeo AB, Shiku H, Takahashi T, John M and Old LJ. (1977). *J. Exp. Med.,* **146,** 720–734.
Dhillon N and Hoekstra MF. (1994). *EMBO J.,* **13,** 2777–2788.
Di Leonardo A, Khan SH, Linke SP, Greco V, Seidita G and Wahl GM. (1997). *Cancer Res.,* **57,** 1013–1019.
Dobles M, Liberal V, Scott ML, Benezra R and Sorger PK. (2000). *Cell,* **101,** 635–645.
Dumaz N, Milne DM and Meek DW. (1999). *FEBS Lett.,* **463,** 312–316.
Endow SA, Chandra R, Komma DJ, Yamamoto AH and Salmon ED. (1994). *J. Cell. Sci.,* **107,** 859–867.
Fish KJ, Cegielska A, Getman ME, Landes GM and Virshup DM. (1995). *J. Biol. Chem.,* **270,** 14875–14883.
Fujikawa-Yamamoto K, Zong ZP, Murakami M, Odashima S, Ikeda T and Yoshitake Y. (1997). *Cell Struct Funct.,* **22,** 399–405.
Gaglio T, Saredi A, Bingham JB, Hasbani MJ, Gill SR, Schroer TA and Compton DA. (1996). *J. Cell. Biol.,* **135,** 399–414.
Grässer FA, Scheidtmann KHt, Tuazon PT, Traugh JA and Walter G. (1988). *Virology,* **165,** 13–22.
Graves PR, Haas DW, Hagedorn CH, DePaoli-Roach AA and Roach PJ. (1993). *J. Biol. Chem.,* **268,** 6394–6401.
Graves PR and Roach PJ. (1995). *J. Biol. Chem.,* **270,** 21689–21694.
Gross SD and Anderson RA. (1998). *Cell Signal,* **10,** 699–711.
Gross SD, Simerly C, Schatten G and Anderson RA. (1997). *J. Cell. Sci.,* **110,** 3083–3090.
Gualberto A, Aldape K and Kozakiewicz K. (1998). *Proc. Natl. Acad. Sci. USA,* **95,** 5166–5171.
Higashimoto Y, Saito S, Tong XH, Hong A, Sakaguchi K, Appella E and Anderson CW. (2000). *J. Biol. Chem.,* **275,** 23199–23203.
Hoekstra MF, Liskay RM, Ou AC, DeMaggio AJ, Burbee DG and Heffron F. (1991). *Science,* **253,** 1031–1034.
Kastan MB, Onyekwere O, Sidransky D, Vogelstein B and Craig RW. (1991). *Cancer Res.,* **51,** 6304–6311.
Khan SH and Wahl GM. (1998). *Cancer Res.,* **58,** 396–401.
Knippschild U, Kolzau T and Deppert W. (1995). *Oncogene,* **11,** 683–690.
Knippschild U, Milne DM, Campbell LE, DeMaggio AJ, Christenson E, Hoekstra MF and Meek DW. (1997). *Oncogene,* **15,** 1727–1736.
Kuret J, Johnson GS, Cha D, Christenson ER, DeMaggio AJ and Hoekstra MF. (1997). *J. Neurochem.,* **69,** 2506–2515.
Lanni JS and Jacks T. (1998). *Mol. Cell. Biol.,* **18,** 1055–1064.
Lehner CF and O'Farrell PH. (1989). *Cell,* **56,** 957–968.
Longenecker KL, Roach PJ and Hurley TD. (1998). *Acta Crystallogr. D. Biol. Crystallogr.,* **54,** 473–475.
Mashhoon N, DeMaggio AJ, Tereshko V, Bergmeier SC, Egli M, Hoekstra MF and Kuret J. (2000). *J. Biol. Chem.,* **275,** 20052–20060.
Milne DM, Palmer RH, Campbell DG and Meek DW. (1992a). *Oncogene,* **7,** 1361–1369.
Milne DM, Palmer RH, Campbell DG and Meek DW. (1992b). *Oncogene,* **7,** 1361–1369.
Minn AJ, Boise LH and Thompson CB. (1996). *Genes Dev.,* **10,** 2621–2631.
Mountain V and Compton DA. (2000). *Anat. Rec.,* **261,** 14–24.
Notterman D, Young S, Wainger B and Levine AJ. (1998). *Oncogene,* **17,** 2743–2751.
Otto A and Deppert W. (1993). *Oncogene,* **8,** 2591–2603.
Palazzo RE, Vaisberg EA, Weiss DG, Kuznetsov SA and Steffen W. (1999). *J. Cell. Sci.,* **112,** 1291–1302.
Roberts JR, Allison DC, Donehower RC and Rowinsky EK. (1990). *Cancer Res.,* **50,** 710–716.

Rowles J, Slaughter C, Moomaw C, Hsu J and Cobb MH. (1991). *Proc. Natl. Acad. Sci. USA,* **88,** 9548–9552.
Sablina AA, Ilyinskaya GV, Rubtsova SN, Agapova LS, Chumakov PM and Kopnin BP. (1998). *J. Cell. Sci.,* **111,** 977–984.
Sakaguchi K, Saito S, Higashimoto Y, Roy S, Anderson CW and Appella E. (2000). *J. Biol. Chem.,* **275,** 9278–9283.
Santos JA, Logarinho E, Tapia C, Allende CC, Allende JE and Sunkel CE. (1996). *J. Cell. Sci.,* **109,** 1847–1856.
Sato N, Mizumoto K, Nakamura M and Tanaka M. (2000). *Exp. Cell. Res.,* **255,** 321–326.
Sharp DJ, Yu KR, Sisson JC, Sullivan W and Scholey JM. (1999). *Nat. Cell. Biol.,* **1,** 51–54.
Simkowski KW and Tao M. (1980). *J. Biol. Chem.,* **255,** 6456–6461.
Singh TJ, Akatsuka A, Blake KR and Huang KP. (1983). *Arch. Biochem. Biophys.,* **220,** 615–622.
Singh TJ, Grundke-Iqbal I and Iqbal K. (1995). *J. Neurochem.,* **64,** 1420–1423.
Thomas NS, Burke LC, Bybee A and Linch DC. (1991). *Oncogene,* **6,** 317–322.
Vaidya AB, Lasfargues EY, Sheffield JB and Coutinho WG. (1978). *Virology,* **90,** 12–22.
Vandre DD and Borisy GG. (1989). *J. Cell. Sci.,* **94,** 245–258.
Vermes I, Haanen C, Steffens-Nakken H and Reutelingsperger C. (1995). *J. Immunol. Methods,* **184,** 39–51.
Wahl AF, Donaldson KL, Fairchild C, Lee FY, Foster SA, Demers GW and Galloway DA. (1996a). *Nat. Med.,* **2,** 72–79.
Wahl AF, Donaldson KL, Fairchild C, Lee FYF, Foster SA, Demers GW and Galloway DA. (1996b). *Nature Med.,* **2,** 72–79.
Walczak CE, Vernos I, Mitchison TJ, Karsenti E and Heald R. (1998). *Curr. Biol.,* **8,** 903–913.
Walker DH and Maller JL. (1991). *Nature,* **354,** 314–317.
Woods CM, Zhu J, McQueney PA, Bollag D and Lazarides E. (1995). *Mol. Med.,* **1,** 506–526.
Yang P and Sale WS. (2000). *J. Biol. Chem.,* **275,** 18905–18912.
Zhai L, Graves PR, Robinson LC, Italiano M, Culbertson MR, Rowles J, Cobb MH, DePaoli-Roach AA and Roach PJ. (1995). *J. Biol. Chem.,* **270,** 12717–12724.